Neutron-Diffraction Study of $NdFe_2Si_2$

H. Pinto and H. Shaked
Nuclear Research Center Negev, P.O.B. 9001, Beer Sheva, Israel
(Received 13 July 1972; revised manuscript received 5 October 1972)

A powder sample of the compound $NdFe_2Si_2$ was studied by neutron diffraction. The compound is found to be isostructural to the analogous actinide compounds AFe_2Si_2, with $I4/mmm$ as a probable space group and ($2a$; $4d$; $4e$) as ionic positions. The bimolecular unit cell consistent with the room temperature (RT) pattern has the dimensions $a = 3.983$ Å, and $c = 10.03$ Å. A least-squares analysis of 20 lines in the RT pattern yielded a weighted R factor of about 9% for two different distributions of the ions: (a) (Nd; Fe; Si); (b) [Nd; $(1-e)$Fe eSi; $(1-e)$Si eFe] with $e = 9.8\%$. The refined z parameter is 0.372 for the two distributions. Five superlattice lines were observed in the 4.2 °K pattern. These lines are consistent with a doubling of the unit cell in the c direction. These lines are inconsistent with any collinear magnetic structure of tetragonal symmetry of the Fe ($4d$) sublattice but are consistent with an antiferromagnetic structure of the Nd ($2a$) sublattice. The structure consists of ferromagnetic sheets perpendicular to c with the magnetic axis along c. These sheets are stacked according to the sequence $++--$. This structure belongs to the magnetic space group $P_{2c}4/nm'm'$. The magnetic moment consistent with the diffracted intensities is $(3.1 \pm 0.3)\mu_B$ per Nd ion. The Néel temperature, $T_N \sim 15.6$ °K, was determined from the intensity-temperature curve of the strongest superlattice line. This line exhibits a smooth temperature dependence but falls considerably above the (Nd^{3+}) $J = \frac{9}{2}$ Brillouin curve.

I. INTRODUCTION

It was suggested[1] that $NdFe_2Si_2$ is isostructural to many other AB_2X_2 (A = U, Th; B = Mn, Fe, Co, Ni, Cu; X = Si, Ge) compounds[2,3] which crystallize in the $BaAl_4$-type structure. This structure belongs to the tetragonal space group D_{4h}^{17}-$I4/mmm$, and in these AB_2X_2 compounds the lattice constants are approximately $a = 4$ Å and $c = 10$ Å. The ions A, B, and X occupy the $2a$, $4d$, and $4e$ positions in this space group. Preliminary studies of the magnetic properties of a powder sample of $NdFe_2Si_2$ have shown[1,4] that it was weakly ferromagnetic at $1.5\ °K < T < T_c$ with $T_c \sim 690$ °K. A paramagnetic-to-antiferromagnetic transition was observed at $T_N \sim 16$ °K in these studies.

In the present paper we report the results of a neutron-diffraction study of a powder sample of $NdFe_2Si_2$ undertaken in order to determine the magnetic structure of this compound.

II. EXPERIMENTAL

The powder sample[5] was prepared using a method similar to the one described in the literature.[6] Neutron ($\lambda \sim 1.02$ Å)-diffraction patterns were taken at 650 and 300 °K (room temperature) and 4.2 °K (liquid-helium temperature). The room-temperature (RT) and liquid-helium-temperature (LHeT) patterns are shown in Fig. 1. The unit cell corresponding to the RT pattern is[7] given by $a = 3.983$ Å and $c = 10.03$ Å. There are two weak lines at $2\theta = 26.0°$ and 30.8°, which are noncomensurate with this unit cell. It is believed that these lines result from small amounts of material other than $NdFe_2Si_2$ present in the sample. In the LHeT pattern, there are three superlattice lines. These lines are indexed on a magnetic unit cell given[7] by $a' = 3.980$ Å and $c' = 19.90$ Å [that is, roughly (a, a, $2c$)] as {011}, {013}, and {015} + {111}. The peak intensity–temperature curve of the line {011} is shown in Fig. 2. This line exhibits a transition-to-magnetic order at about 15.6 °K in agreement with the measurements[1,4] mentioned in Sec. I.

III. CRYSTALLOGRAPHIC STRUCTURE

Nuclear intensities were calculated for the structure shown in Fig. 3. The space group $I4/mmm$ with Nd, $(1-e)$Fe + eSi and eFe + $(1-e)$Si at the positions $2a$, $4d$, and $4e$, respectively, was used (Table I). The possibility of a mixture of the B and the X (Fe and Si in our case) ions among the $4d$ and $4e$ positions was previously mentioned[6] and is considered here. The parameters e, z, and the Debye–Waller constant B (see Appendix A) were refined to give a best fit (least squares) of the calculated to the observed integrated intensities. The refined parameters with the corresponding weighted R factors[8] are given in Table II. The first set was

TABLE I. Ionic positions in $NdFe_2Si_2$, space group $I4/mmm$.

Position	Coordinates + ($\frac{1}{2}$, $\frac{1}{2}$, $\frac{1}{2}$)	Ions ($0 < e < 1$)
$2a$	0 0 0	Nd
$4d$	0 $\frac{1}{2}$ $\frac{1}{4}$, $\frac{1}{2}$ 0 $\frac{1}{4}$	$(1-e)$ Fe + eSi
$4e$	0 0 z, 0 0 $\bar{z}$	$(1-e)$ Si + eFe

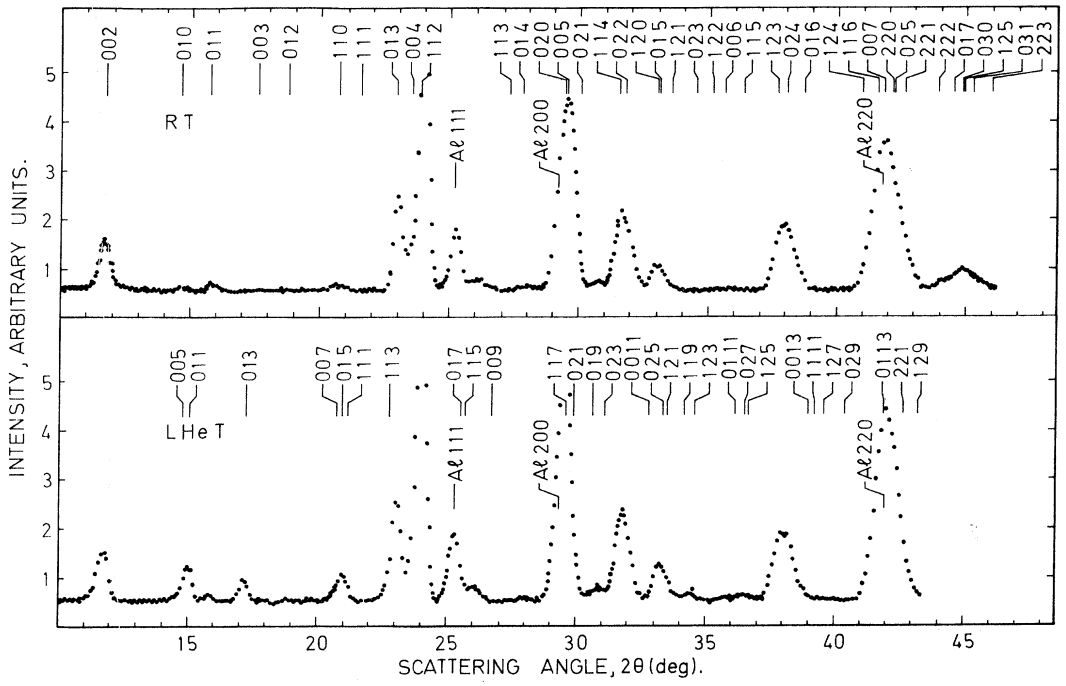

FIG. 1. Neutron ($\lambda \sim 1.02$ Å)-diffraction patterns of $NdFe_2Si_2$ at RT and at LHeT. The RT and the LHeT patterns were indexed according to $a = 3.983$ Å, $c = 10.03$ Å and $a' = 3.980$ Å, $c' = 19.90$ Å, respectively.

obtained when e was fixed at 0, whereas, the second set was obtained with e allowed to vary. The calculated intensities for the two sets together with the observed integrated intensities are given in Table III.

IV. MAGNETIC STRUCTURE

Magnetization measurements of a powder sample of $NdFe_2Si_2$ have shown[1,4] that it has a weak ferromagnetic moment at $1.5\ ^\circ\text{K} < T < T_C$ with $T_C \sim 690\ ^\circ\text{K}$. The possibility of magnetic structure at RT must therefore be discussed first.

The contribution of weak ferromagnetism (wf) to neutron reflections is too small to be measured. If, on the other hand, the wf were associated with antiferromagnetism, as is usually the case,[9] we would expect to observe magnetic contributions to neutron reflections. Suppose that this is the case here and we do have such a contribution at RT. At 650 °K, where $T/T_C \sim 650/690 \sim 0.94$, this contribution must then decrease to less than 10% of its RT value. As already mentioned, our 650 °K pattern is essentially unchanged from the RT pattern,

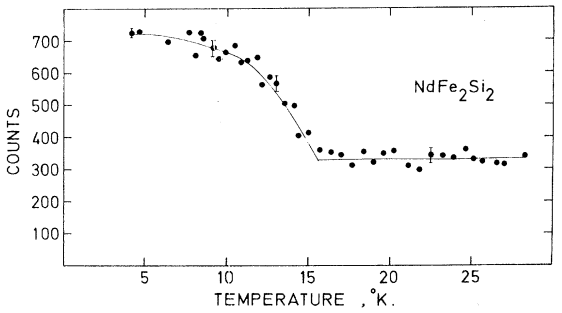

FIG. 2. Peak intensity–temperature curve of the magnetic {011} line.

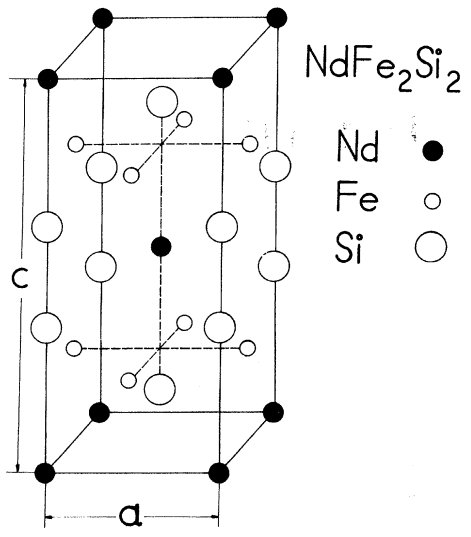

FIG. 3. Crystallographic structure of $NdFe_2Si_2$. One crystallographic unit cell is shown.

TABLE II. Refined parameters.

e(%)	z	B (Å^2)	R (%)
0	0.372±0.002	0.0±0.4	9.71
9.80±0.04	0.372±0.002	0.4±0.4	8.32

and no such decrease is observed. We therefore conclude that a collinear magnetic structure of the localized type, where the Nd and/or Fe sublattice consists of localized magnetic moments that are greater than $1\mu_B$, does not exist at RT. There is some support to this conclusion in the RT Mössbauer spectrum of the Fe ion in this compound. The spectrum shows[10] isomeric shift similar to the one found in metallic iron but shows no Zeeman splitting.

We shall next determine the magnetic structure at LHeT. We have already established (Sec. II) that the magnetic unit cell is approximately (a, a, $2c$). The magnetic reflections identified in the LHeT pattern are the superlattice lines {011}, {013}, {015}+{111}, and a trace of {113}, which is largely obscured by the nuclear reflection {013}. With the aid of diffraction patterns taken with long-wavelength ($\lambda \sim 2.4$ Å; Fig. 4) neutrons we were

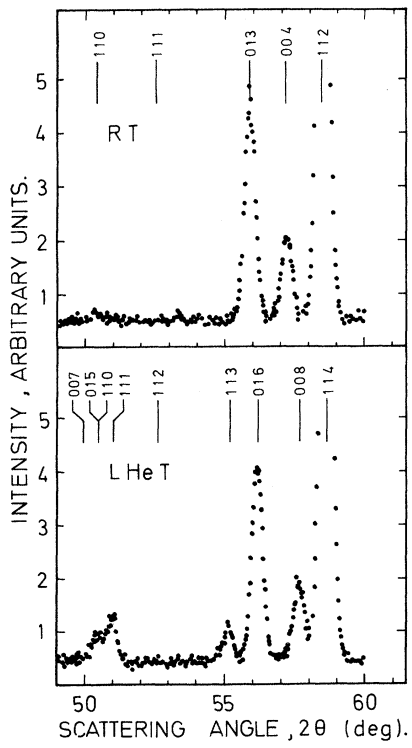

FIG. 4. Neutron ($\lambda \sim 2.4$ Å)-diffraction patterns of $NdFe_2Si_2$ at RT and at LHeT. The RT and the LHeT patterns were indexed according to $a = 3.983$ Å, $c = 10.03$ Å and $a' = 3.980$ Å, $c' = 19.90$ Å, respectively.

able to resolve the last two lines so that we have altogether the five magnetic reflections {011}, {013}, {015}, {111}, and {113}. We look now for a collinear magnetic structure of the highest symmetry (tetragonal) which will account for these five lines. There are only four possible configurations with antitranslation along c and which have tetragonal symmetry on the Fe sublattice. The four respective structure factors are given by

$$(1 \pm e^{\pi i (h+k)})(1 \pm e^{\pi i l/2})(1 - e^{\pi i l}).$$

Every one of these structure factors vanishes for either $h+k=2n$ or $h+k=2n+1$. Hence, out of the four possible magnetic configurations no single configuration can account for the appearance of all five lines. This leads to the conclusion that all collinear structures of tetragonal symmetry on the Fe sublattice are inconsistent with our LHeT pattern. A collinear structure of orthorhombic symmetry which is consistent with our LHeT pattern is described in Appendix B. We next investigate the possible configurations which have tetragonal symmetry on the Nd sublattice. There are only two such configurations, whose structure factors are given by

$$(1 \pm e^{\pi i (h+k+l/2)})(1 - e^{\pi i l}).$$

For $l = 2n+1$ there is no condition on $h+k$. Furthermore, the absolute values of the two structure factors are identical for all hkl; hence, the two configurations must be equivalent. Indeed, one configuration is transformed into the other through a body-center translation of the crystallographic lattice. The absence of the {001}, {003}, and {005} lines in the LHeT pattern implies that the

TABLE III. Nuclear lines. Comparison of calculated and observed integrated intensities in the RT pattern of $NdFe_2Si_2$. The calculated intensities were obtained using the refined parameters (Table II).

No.	{hkl}	$I_{obs} \pm \sigma$	I_{calc} $e=0.0\%$	I_{calc} $e=9.8\%$
1	001	0 ± 200	0	0
2	002	12700 ± 400	14565	13815
3	010	0 ± 200	0	0
4	011	1000 ± 400	412	250
5	003	0 ± 200	0	0
6	012	0 ± 200	0	0
7	110	500 ± 400	746	240
8	111	0 ± 200	0	0
9	013	20900 ± 800	19238	22440
10	004, 112	78500 ± 800	74136	74278
11	113	0 ± 200	0	0
12	014	300 ± 300	0	0
13	114, 022	30000 ± 800	32090	31573
14	120, 015, 121	8800 ± 600	8644	9589
15	023	0 ± 200	0	0
16	122	0 ± 200	0	0
17	006	200 ± 200	1387	1183
18	115	0 ± 200	0	0
19	123, 024, 016	29500 ± 600	28368	28139
20	222, 017, 030, 125, 031, 223	12200 ± 800	14602	14408

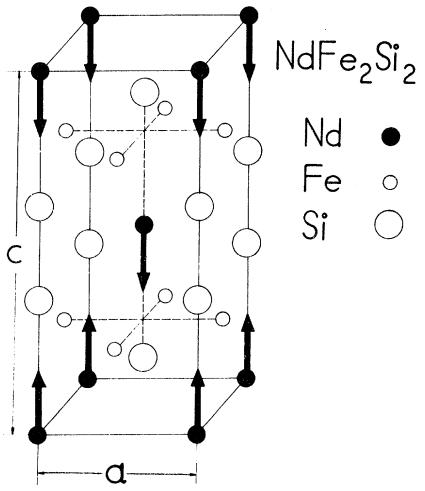

FIG. 5. Magnetic structure of $NdFe_2Si_2$ at LHeT. Only half of the magnetic unit cell is shown.

antiferromagnetic axis is along $\hat{c}$. These arguments are sufficient for making the following statement: The only collinear magnetic structure of tetragonal symmetry on one of the two sublattices which accounts for the appearance of the five magnetic lines is the one shown in Fig. 5. A comparison of the relative intensities calculated (see Appendix A) for this structure with the observed integrated intensities of these five lines is given in Table IV. The intensities compare very well and we conclude that the structure shown in Fig. 5 is the only collinear structure of tetragonal symmetry which is consistent with our LHeT pattern. The magnetic space group of this structure is $P_{2c}4/nm'm'$ in the western notation[11] and $III^{432}_{130} - P_c4/ncc$ in the eastern notation.[12] The number of Bohr magnetons per Nd ion calculated (see Appendix A) from the LHeT pattern is $(3.1 \pm 0.3)\mu_B$. The expected value[13] for $Nd^{3+}(^4I_{9/2})$ is $gJ = 3.2\mu_B$.

V. DISCUSSION

The proposed magnetic structure (Fig. 5) has two unexpected features. (i) It is the Nd sublattice which orders magnetically and not the much denser Fe sublattice. (ii) Consider the three layers perpendicular to $\hat{c}$ of Nd ions (Fig. 5) at $z = 0$, $\frac{1}{2}$, and 1. The pair of layers $0-\frac{1}{2}$ is crystallographically equivalent to the pair $\frac{1}{2}-1$. One would therefore expect the same magnetic interaction in the two pairs. In the proposed structure one pair of layers couples antiferromagnetically whereas the other pair couples ferromagnetically in contradiction to what was expected. As far as we know,[14,15] UAs and $UP_{1-x}S_x$ with $0 < x < 0.1$ are the only compounds which, at low temperature, order in such a structure which was classified[16] as fcc type IA. We offer no explanation to the first feature except to mention that from the Mössbauer spectrum below T_N it is estimated[10] that the internal magnetic field on the Fe nuclei is 30 kG. It is reasonable to expect that this relatively low field is a consequence of the ordering of the Nd sublattice. In regard to the second feature we make the following comment: If the coupling between next-nearest layers is antiferromagnetic and is much stronger than the coupling between nearest layers then the proposed structure will result. This is independent of whether the interaction between nearest layers is ferromagnetic or antiferromagnetic. This situation implies that the 180° antiferromagnetic interaction between the two Nd ions 10 Å apart through the pair of Si ions is much stronger than the 120° interaction between the two Nd ions 6 Å apart. It is difficult to see how a simple superexchange can be responsible

TABLE IV. Magnetic reflections. Comparison of calculated and observed relative integrated intensities. The intensities were calculated for the magnetic structure shown in Fig. 5.

$\{hkl\}$ [a]	$I_{obs} \pm \sigma$	I_{calc} [b]
011	348 ± 39	367
013	247 ± 26	212
015	85 ± 14	96
111	166 ± 20	180
113	153 ± 18	144

[a]Indices are given with respect to the magnetic unit cell.

[b]With $B = 0$.

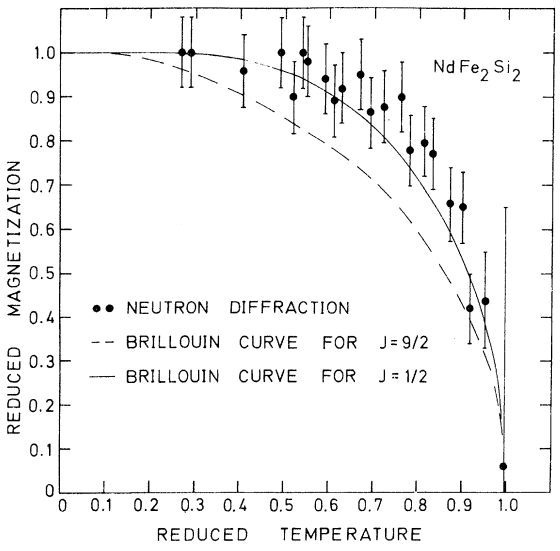

FIG. 6. Reduced temperature dependence of the sublattice magnetization of $NdFe_2Si_2$ derived from the magnetic line {001}, compared with results of molecular-field theory with $J = \frac{1}{2}$ and $\frac{9}{2}$.

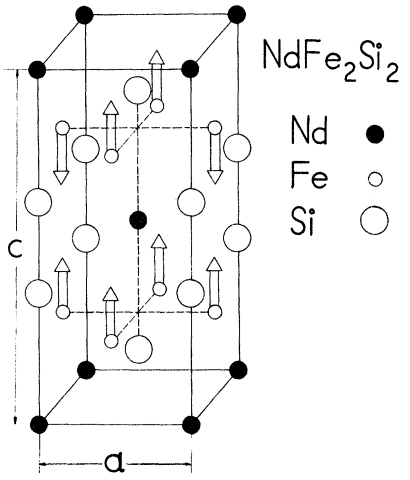

FIG. 7. Low-symmetry magnetic structure of the Fe sublattice which is consistent with the neutron-diffraction data (see Appendix B). Only half of the magnetic unit cell is shown.

for such a behavior. It was suggested[15] in the case of UAs that the dominant interaction is of the Ruderman–Kittel–Yosida (RKY) type. Since $NdFe_2Si_2$ is an electrical conductor,[1] it is quite possible that the RKY interaction plays a similar role in this compound.

The Nd sublattice transforms from an I lattice $[\frac{1}{2}(\bar{a},a,c),\ \frac{1}{2}(a,\bar{a},c),\ \frac{1}{2}(a,a,\bar{c})]$ in the paramagnetic state to a P_{2c} lattice $[(a,0,0),\ (0,a,0),\ (0,0,c)']$ in the antiferromagnetic state. The $\vec{k}$ vector for this transition is $(0,0,\pi/c)$ and lies inside the Brillouin zone. Hence, it can be shown[17,18] that this transition is not allowed as a second-order phase transition. In this connection, the sublattice magnetization was calculated from the temperature dependence of the peak intensity of the magnetic line $\{011\}$ (Fig. 2). The results are compared in Fig. 6 with the magnetization M/M_0, calculated in the molecular-field model from the equation

$$M/M_0 = B_J[(T/T_N)(M/M_0)] \quad \text{for } J=\tfrac{1}{2},\tfrac{9}{2}.$$

As temperature decreases, the buildup of sublattice magnetization is considerably sharper than predicted by molecular-field $[J(Nd^{3+})=\frac{9}{2}]$ theory. Hence, in view of this result and the theoretical consideration mentioned above, the transition is probably not of the second order.

ACKNOWLEDGMENTS

The authors are indebted to Dr. I. Meyer for suggesting the problem, supplying the sample, and for many discussions. Discussions with Dr. S. Goshen and D. Mukamel of our laboratory and with I. Felner, Dr. R. Bauminger, Professor S. Ofer, and Professor M. Schieber are greatly appreciated.

APPENDIX A

The calculated intensity is given[13] by

$$I_{calc}(hkl) = q^2 j F^2 f^2 p^2 e^{-2B(\sin\theta/\lambda)^2}/\sin\theta\sin2\theta.$$

For the nuclear reflections $(qfp=1)$ we have used[19] 0.72, 0.95, and 0.42 for the scattering amplitudes (in units of 10^{-12} cm) of Nd, Fe, and Si, respectively. In the magnetic reflections we have used[20] $f = \exp[-1.94(\sin\theta/\lambda)^2]$ for the form factor of Nd^{3+}.

To obtain the number of Bohr magnetons μ we have used

$$I_{obs}(011) = 9075 \pm 300,$$

$$I_{obs}(002) = 14345 \pm 400,$$

$$I_{calc}(011) = 1673p^2,$$

and

$$I_{calc}(002) = 1867$$

in the equality

$$I_{calc}(011)/I_{obs}(011) = I_{calc}(002)/I_{obs}(002).$$

Setting $p = 0.27\mu_B$ (in units of 10^{-12} cm) in this equality we obtained $\mu = 3.1 \pm 0.3\mu_B$.

APPENDIX B

There is a collinear magnetic structure of orthorhombic symmetry on the Fe sublattice which is consistent with the diffraction pattern. This structure (Fig. 7) belongs to the space group $P_{2c}m'm'n$ which is not a maximal subgroup[21] of $1'I4/mmm$. The number of Bohr magnetons per Fe ion calculated for this structure from the LHeT pattern is $(1.5 \pm 0.2)\mu_B$. The reduction in symmetry corresponding to $1'I4/mmm \rightarrow P_{2c}m'm'n$ is 8, whereas, the reduction corresponding to $1'I4/mmm \rightarrow P_{2c}4/nm'm'$ is only 4. Furthermore, such a structure on the Fe sublattice is inconsistent with the low field (30 kG) observed[10] on the iron nuclei.

---

[1] I. Meyer and I. Felner (private communication).

[2] Z. Ban and M. Sikirica, Z. Anorg. Allgem. Chem. 356, 96 (1967).

[3] W. Rieger and W. Parthe, Mh. Chem. 100, 444 (1969).

[4] M. M. Schieber (private communication).

[5] The sample was prepared and supplied to us by I. Meyer.

[6] L. Omejec and Z. Ban, Z. Anorg. Allgem. Chem. 380, 111 (1971).

[7] Deduced from the pattern taken with long-wavelength neutrons ($\lambda \sim 2.4$ Å), see Sec. IV.

[8] The weighted R factor is given by $R = \{\Sigma[(I_{obs} - I_{calc})/\sigma]^2/\Sigma(I_{obs}/\sigma)^2\}^{1/2}$, where σ's are the estimated errors in

I_{obs} (listed in Table III).
[9]T. Moriya, in *Magnetism*, edited by G. T. Rado and H. Suhl (Academic, New York, 1965), Vol. I.
[10]R. Bauminger and S. Ofer (private communication).
[11]W. Opechowski and R. Guccione, in *Magnetism*, edited by G. T. Rado and H. Suhl (Academic, New York, 1965), Vol. II a.
[12]V. A. Koptsik, *Shubnikov Groups* (Moscow State U. P., Moscow, 1965)(in Russian).
[13]G. W. Bacon, *Neutron Diffraction*, 2nd ed. (Oxford U. P., Oxford, England, 1962).
[14]J. Leciejewicz, R. Troc, A. Murasik, and A. Zygmunt, Phys. Status Solidi 22, 517 (1967).
[15]G. H. Lander, M. Kuznietz, and Y. Baskin, Solid State Commun. 6, 877 (1968).
[16]D. E. Cox, Brookhaven National Laboratory Rept. No. BNL 13822, June, 1969 (unpublished).
[17]G. Y. Lyubarskii, *The Application of Group Theory in Physics* (Pergamon, New York, 1960).
[18]E. M. Lifshitz, J. Phys. VI 61, 251 (1942).
[19]Neutron Diffraction Commission, Acta Cryst. A28, 357 (1972).
[20]W. C. Koehler and E. O. Wollan, Phys. Rev. 92, 1380 (1953).
[21]J. Neubuser and H. Wondratschek (unpublished).

PHYSICAL REVIEW B VOLUME 7, NUMBER 7 1 APRIL 1973

Strong Correlations in Disordered Systems*

Hidetoshi Fukuyama† and H. Ehrenreich
Division of Engineering and Applied Physics, Harvard University, Cambridge, Massachusetts 02138
(Received 24 October 1972)

The effects of strong correlations in a substitutional binary alloy A_xB_{1-x} having a single nondegenerate tight-binding band are examined by use of the coherent-potential approximation and the alloy analogy of Hubbard to treat the effects of disorder and Coulomb interactions, respectively. It is shown that there are no ferromagnetic instabilities in the B band for any band structure, carrier number and the concentration of B atoms, if the potential at A atomic sites are assumed to be positive infinite. This assumption causes the A sites to be inaccessible to electrons. Moreover, the spin susceptibility is found to remain finite even if the density of states is vanishing at the Fermi energy in the limit of the half-filled B band.

I. INTRODUCTION

Since the coherent-potential approximation (CPA)[1,2] was proposed, much progress has been made in the theory of alloys based on a one-electron Hamiltonian. Many-body effects, however, have not yet been discussed extensively. Recently, some authors[3-6] examined the itinerant-electron magnetism of a binary alloy of the type A_xB_{1-x} represented by the Hamiltonian

$$\mathcal{H} = \sum_{i,j,\sigma} t_{ij} a^{\dagger}_{i,\sigma} a_{j,\sigma} + \sum_{i,\sigma} \epsilon^0_i n_{i,\sigma} + \sum_i U_i n_{i,\sigma} n_{i,-\sigma} , \tag{1.1}$$

where $a_{i,\sigma}(a^{\dagger}_{i,\sigma})$ is the annihilation (creation) operator of an electron with spin σ at the ith Wannier site. ϵ^0_i and U_i are assumed to take on values ϵ^0_A, ϵ^0_B and U_A, U_B, respectively.

Hasegawa and Kanamori[3] and Levin *et al.*[4] treated the last term in Eq. (1.1) in the *local* Hartree approximation by writing the atomic energy in the form

$$\epsilon_{i,\sigma} = \epsilon^0_i + U_i \langle n_{i,-\sigma} \rangle . \tag{1.2}$$

In Eq. (1.2), $\langle n_{i,-\sigma} \rangle$ is the average electron number with spin σ at the ith site, which is to be determined self-consistently. They applied the CPA to $\epsilon_{i,\sigma}$. Reference 6 uses this scheme to discuss the dynamical spin susceptibility.

Equation (1.2) is reasonable when the Coulomb interactions are moderately weak. However, as is known, there exist real systems in which the Coulomb forces and therefore the electron correlations are strong. The case of impurity-band conduction in weakly doped uncompensated semiconductors[7] and the alloy of transition-metal oxides[8] are examples. The latter were treated recently by Rice and Brinkman.[9]

The present understanding of the effects of strong correlations is not yet satisfactory even in pure systems. However, the investigations by Hubbard[10] have yielded valuable qualitative insight into this problem. He argues that, if the correlations are sufficiently strong, the quasiparticle energy spectrum has a gap corresponding to the double occupancy of the same site. He identified this gap with the onset of the Mott transition. This type of gap is also expected in alloy systems. Thus two different kinds of gaps will exist in alloys which arise, respectively, from disorder and correlations.

As was shown in Ref. 2, one of the essential parts of Hubbard's approximations, the so-called "scattering correction" in his terminology, is equivalent to the CPA. At a fixed instant in time, the electrons with opposite spins are regarded as